



# Optimization of a Mixture of Curcuma Dye Mixture with SiO<sub>2</sub> (Rice Husk Waste) to the Energy Efficiency of TiO<sub>2</sub> - based Solar Cells

Tulus Subagyo\*, Denny Widhiyanuriyawan, Agung Sugeng Widodo, and I Nyoman Gede Wardana

Received : April 22, 2025

Revised : June 14, 2025

Accepted : July 1, 2025

Online : July 29, 2025

## Abstract

Global energy challenges and environmental problems encourage the search for sustainable energy solutions, with TiO<sub>2</sub>-based solar cells that are still limited to its efficiency due to low light absorption and charge recombination. This study aims to examine the synergistic effect of curcuma and SiO<sub>2</sub> dye from rice husk waste in improving the energy efficiency of TiO<sub>2</sub> solar cells. The research methodology involves the fabrication of sensitive solar cells with different layer compositions: TiO<sub>2</sub> only, TiO<sub>2</sub> with one layer of SiO<sub>2</sub> (1L-SiO<sub>2</sub>), two layers (2L-SiO<sub>2</sub>), and three layers (3L-SiO<sub>2</sub>). The TiO<sub>2</sub> photoanode is prepared using the screen printing method, followed by loading coloring through immersion in the curcuma coloring solution. The performance of solar cells is evaluated using the current voltage measurement (I-V) and electrochemical impedance spectroscopy (EIS) to analyze efficiency, charge transportation, and recombination processes. The results show that the addition of SiO<sub>2</sub> increases the efficiency of solar cells, with 1L-SiO<sub>2</sub> producing the highest compilation of short circuit ( $J_{sc}$ ) 0.37 mA/cm<sup>2</sup>, showing an increase in cargo transportation. However, 1L-SiO<sub>2</sub> shows a decrease in performance due to excessive thickness, which leads to an increase in charge recombination and internal resistance. Impedance analysis confirms that 1L-SiO<sub>2</sub> optimizes cargo transportation but also increases recombination resistance, which affects overall efficiency. Adding SiO<sub>2</sub> from rice husk waste increases the efficiency of TiO<sub>2</sub>-based solar cells, with curcuma coloring increases light absorption and charge transfer. However, excessive SiO<sub>2</sub> layers reduce performance due to higher recombination and resistance. Further research is needed to optimize the thickness of the layer and dye stability.

**Keywords:** TiO<sub>2</sub>, solar cells, sensitive solar cells, curcuma coloring, SiO<sub>2</sub>, rice husk waste

## 1. INTRODUCTION

The development of sustainable and efficient solar cells is one of the most promising approaches to meet global energy demand while overcoming environmental problems. Solar cells based on titanium dioxide (TiO<sub>2</sub>), especially solar-sensitive solar cells (DSSC), have gathered significant attention due to low costs, ease of fabrication, and relatively high efficiency [1]-[4]. However, its efficiency is still limited by factors such as light absorption and charge recombination [5]. Therefore, various strategies have been explored to improve the performance of TiO<sub>2</sub>-based solar cells, one of which is the use of natural dyes.

Curcuma, a plant genus that is widely used in treatment and traditional food, contains curcumin,

bioactive compounds known for antioxidant and anti-inflammatory properties [6][7]. Recent studies have shown the potential of curcuma-based dyes in improving the ability to harvest solar cell light [8] [9]. This natural dyes are environmentally friendly alternatives for synthetic dyes, which are often toxic and expensive [10]. The integration of curcuma coloring in TiO<sub>2</sub>-based solar cells can help increase their light absorption and, as a result, their overall energy efficiency [11].

One of the promising ingredients to improve the performance of solar cells is silica (SiO<sub>2</sub>) originating from rice husk waste. The husk constellation, abundant agricultural products, is rich in SiO<sub>2</sub>, which can be used to improve structural and optical properties of solar cell electrodes [12] [13]. The latest progress has shown that SiO<sub>2</sub> can increase the surface area and porosity of TiO<sub>2</sub> electrodes, thereby increasing the absorption of light and the efficiency of electron transportation [14]. Utilization of SiO<sub>2</sub> from rice husk waste not only provides effective materials to improve the performance of solar cells but also offers sustainable solutions for disposal of agricultural waste [15][16]. The combination of curcuma and SiO<sub>2</sub> coloring (from rice husk waste) in TiO<sub>2</sub>-based solar cells has the potential to optimize energy efficiency by overcoming limitations associated

## Publisher's Note:

Pandawa Institute stays neutral with regard to jurisdictional claims in published maps and institutional affiliations.



## Copyright:

© 2025 by the author(s).

Licensee Pandawa Institute, Metro, Indonesia. This article is an open access article distributed under the terms and conditions of the Creative Commons Attribution (CC BY) license (<https://creativecommons.org/licenses/by/4.0/>).

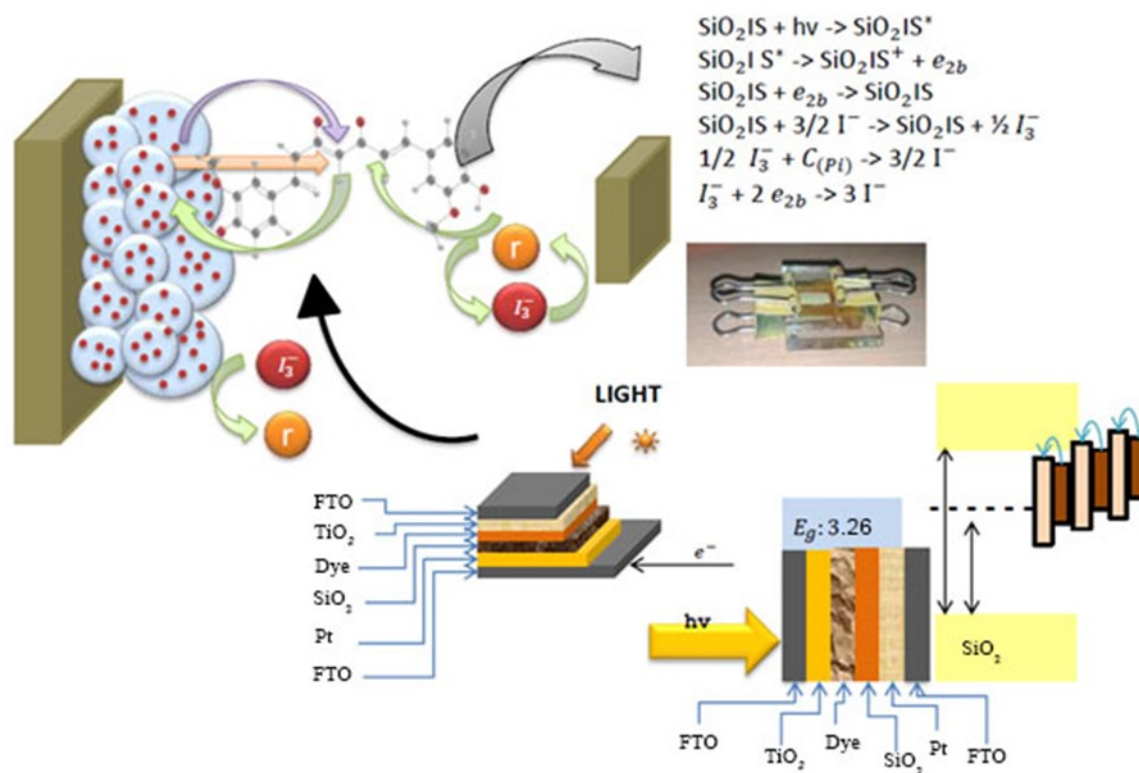


Figure 1. DSSC cell design.

with light absorption, cargo transportation, and material sustainability. This study aims to investigate the synergistic effects of the curcuma coloring mixture with SiO<sub>2</sub> on TiO<sub>2</sub>-based solar cell energy efficiency, with a focus on optimizing the composition of the mixture to achieve the highest DSSC performance.

## 2. MATERIALS AND METHODS

### 2.1. Material

We use an experimental study to optimize the curcuma coloring mixture with SiO<sub>2</sub> (from rice husk waste) to increase the energy efficiency of TiO<sub>2</sub>-based solar cells. The materials used include TiO<sub>2</sub> nanoparticles, curcuma extract, and SiO<sub>2</sub> sourced from rice husk waste. The TiO<sub>2</sub> nanoparticles are bought from Sigma-Aldrich, while curcuma dyes are extracted from the *Curcuma longa* root. Rice husk was collected from a rice factory in Malang, Indonesia. All chemicals and solvents used in experiments are analytical levels, including ethanol and acetone, which is used for washing and preparation.

### 2.2. Curcuma and SiO<sub>2</sub> Coloring Preparations from

#### Rice Husk

##### 2.2.1. Curcuma Coloring Extraction

Curcuma coloring is extracted from the root of the dry *longa* curcuma using an ethanol-based maceration process. Dry root (50 g) is crushed into powder and soaked in 500 mL of 96% ethanol for 72 h. The extract is then filtered, and the solvent is evaporated under reduced pressure using a rotary evaporator to get a concentrated coloring solution. This dyes are used in various concentrations to test their efficiency in improving the performance of TiO<sub>2</sub>-based solar cells [17][18].

##### 2.2.2. SiO<sub>2</sub> Extraction from Rice Husk

The SiO<sub>2</sub> is extracted from rice husks using a simple alkaline treatment method. Rice husk (100 g) was first washed thoroughly with distilled water to remove dirt. Then heated in the oven at 600 °C for 5 h to remove organic content, followed by soaking in a 2 M NaOH solution for 24 h. After filtering and washing with distilled water, the remaining SiO<sub>2</sub> is dried at 110 °C for 12 h and crushed into fine powder. SiO<sub>2</sub> powder is then characterized using X-ray diffraction (XRD) and scanning electron microscope (SEM) to confirm the

purity and size of the particle, respectively [19][20].

### 2.3. $\text{TiO}_2$ -based Solar Cell Fabrication

The research method used is a laboratory experiment with the independent variable in the form of variations in the thickness of the  $\text{TiO}_2$  photoactive layer, which is an integral part of the structure of the photographic material in the DSSC. In the initial stages, the blocking layer is applied to the conductive glass substrate of fluorine-doped tin oxide (FTO) using spin coating techniques to ensure homogeneous and controlled deposition. After that, the  $\text{TiO}_2$  layer is deposited using the T-61 Pasta Printing method, with a variety of thickness regulated based on the number of layers, namely as many as 1 layer, 2 and 3 layers. Furthermore, an additional reflective layer deposition above the mesoporous  $\text{TiO}_2$  layer uses the same screen-printing method, with the aim of increasing light reflection for more optimal

absorption efficiency.

The next process involves additional treatment by soaking photographs into the titanium tetratoxide acetylacetonate isopropoxide solution that has been dissolved in 2-propanol. After soaking, the photograph is dried in a stable temperature condition of 70 °C for a duration of 30 min to increase the surface characteristics of the material. Loading of natural curcumin in the photograph is done through the immersion method, by soaking it in a solution of curcumin concentrating 0.7 mm for 24 h, to ensure optimal dye adsorption on the  $\text{TiO}_2$  surface.

Furthermore,  $\text{TiO}_2$ -based solar cells are made by preparing  $\text{TiO}_2$  photoanode. Transparent conductive oxide (TCO) glass is cleaned with acetone and isopropanol, followed by treatment with ultraviolet (UV) lamps for 30 min. The  $\text{TiO}_2$  nanoparticles are scattered in ethanol solution and applied to TCO glass with a doctor's blade method, forming a thin

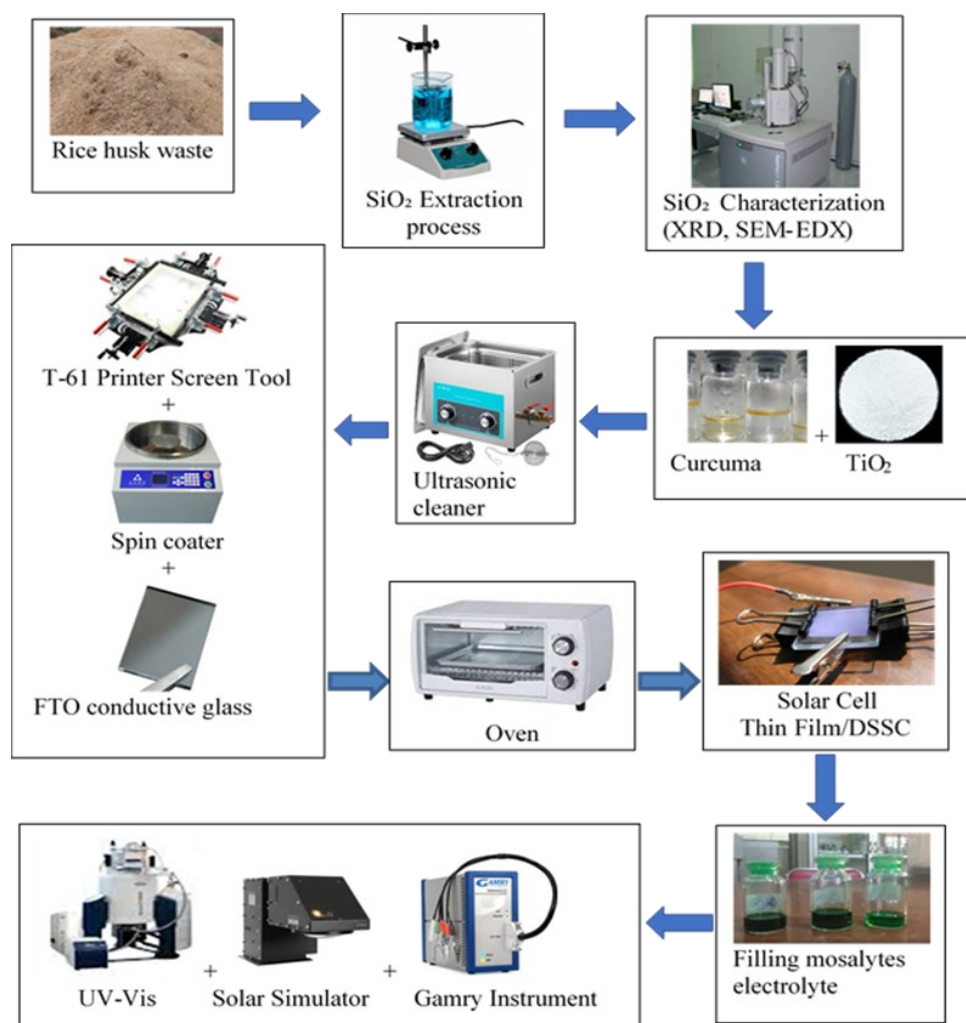


**Figure 2.** Experimental set up.

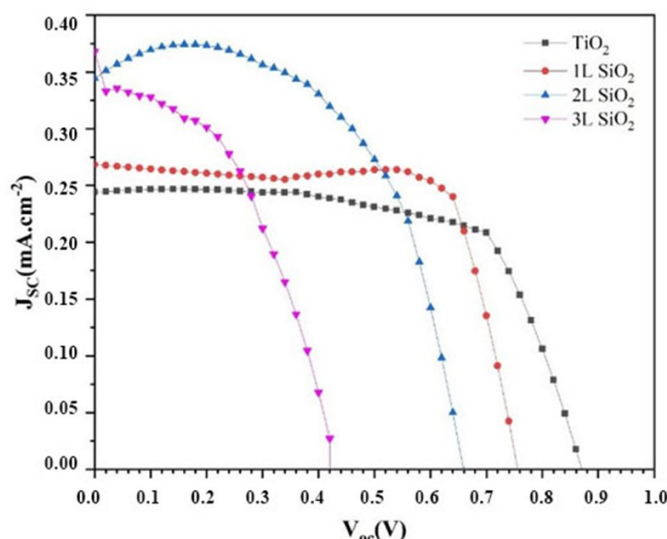


**Figure 3.** Relationship between  $J_{sc}$  and  $V_{oc}$  for various materials.

TiO<sub>2</sub> film. After syntrary at 450 °C for 30 min, TiO<sub>2</sub> films are coated with a mixture of curcuma and SiO<sub>2</sub> coloring (in various weight ratios) to evaluate the effects of optimization on energy efficiency. Cells are then assembled with platinum and electrolyte electrolytes/triiodide electrolytes [21][22]. Complete DSSC components, consisting of modified photographs, iodide electrolytes as electron transfer mediums, spacers from 25 µm sulyn material which functions as an insulator and sealing between layers, as well as opponent's electrodes in the form of platinum (Pt) layers. The component series is assembled with a structural scheme described in more detail in Figure 1.

## 2.4. Characterization of Solar Cell Performance

### 2.4.1. UV-VIS Spectroscopy

To characterize the optical properties of the curcuma coloring mixture, the UV-Vis absorption spectrum is obtained using the Shimadzu UV-3600 spectrophotometer. The absorption spectrum is recorded in the range of 300–800 nm, and the capacity of light absorption from a mixture of coloring compared to pure TiO<sub>2</sub>-based solar cells [23].

### 2.4.2. Current Voltage Measurement (I-V)

TiO<sub>2</sub>-based solar cell energy efficiency is evaluated using the current voltage measurement (I-V). The 2400 Sumber Keithley gauge is used to measure the photocurants in the simulated sunlight

(100 mW/cm<sup>2</sup>) using Xenon lamps. Power conversion efficiency (PCE) of each solar cell is calculated using Equation 1 [24];

$$PCE = \frac{J_{sc} \times V_{oc} \times FF}{P_{in}} \quad (1)$$

where  $J_{sc}$  is a short circuit current density,  $V_{oc}$  is an open circuit voltage, and FF is a filling factor. This experiment was carried out with variations in mixing curcuma and SiO<sub>2</sub> to obtain optimal solar cell performance. This study uses variations in the number of mixture layers, namely 1 layer (1L-SiO<sub>2</sub>), 2 layers (2L-SiO<sub>2</sub>), and 3 layers (3L-SiO<sub>2</sub>) in DSSC solar cells. Where the average thickness of each layer variation is as follows: 1L-SiO<sub>2</sub> ≈ 1.2±0.1 µm, 2L-SiO<sub>2</sub> ≈ 2.4±0.2 µm, and 3L-SiO<sub>2</sub> ≈ 3.6±0.3 µm. This thickness increases proportionally with the number of layers printed using the screen-printing method.

In the early stages, the blocking layer is applied to the conductive glass substrate that is coated in FTO using the spin coating technique, to ensure a homogeneous and controlled deposit. Furthermore, The TiO<sub>2</sub> layer is deposited using the T-61 Paste Screen Printing Method, with a variety of things that is adjusted based on the number of layers. Additional reflective layers are applied above the mesopori layer TiO<sub>2</sub> using the same screen-printing method, with the aim of increasing light reflection and achieving more optimal absorption efficiency. The next process involves immersion of photographs in the tetraetoxide acetylacetonate



isopropoxide solution which has been dissolved in 2-propanol. After immersion, the photo is dried at a stable temperature of 70 °C for 30 min to increase the surface characteristics of the material.

### 2.4.3. Electrochemical Impedance Spectroscopy (EIS)

The capacitance value presented in this study was obtained from the Electrochemical Impedance Spectroscopy (EIS) analysis using the equivalent circuit model approach. Complex impedance spectrum data (nyquist curve) analyzed and fitted using zview software with a simple electrical circuit model (randles circuit), which includes serial resistance elements (RS), charge transfer resistance (RCT), and capacitive elements (CPE or multiple capacitance). The capacitance value ( $C_1$ ) is calculated based on the fitting curve at low frequency, which reflects the ability of the electrode in storing charges before the charge transfer process takes place. Measurements are carried out in a frequency range of 100 kHz to 0.1 Hz with AC signal amplitude of 10 mV in dark conditions at room temperature. This method allows quantitative evaluation of the electrochemical performance of the photographic interface modified by the variation of the  $\text{SiO}_2$  layer. The DSSC performance testing is carried out using a solar simulator integrated with a device for measurement of voltage-voltage characteristics (I-V meter), which aims to determine the efficiency of the DSSC system energy conversion. In addition, the analysis of DSSC internal resistance was also carried out using the

EIS technique to identify the characteristics of electrical resistance in the solar cell device. Experimental settings used in this study are shown in Figure 2.

## 3. RESULTS AND DISCUSSIONS

### 3.1. $\text{SiO}_2$ Layer Thickness on Solar Cell Performance

Figure 3 shows different characteristics related to the density of short circuit current ( $J_{SC}$ ) and open circuit voltage ( $V_{OC}$ ). In  $\text{TiO}_2$  as a reference material, the  $J_{SC}$  value is relatively stable in the range of 0.25 mA/cm<sup>2</sup> at low voltage. However, this material shows a sharp decrease in current when the voltage increases above 0.7 V, which indicates that  $\text{TiO}_2$  has limitations in maintaining current at a higher voltage [25]. This shows that  $\text{TiO}_2$  has a lower charge transfer efficiency compared to other materials tested. Conversely, 1L- $\text{SiO}_2$  material shows an increase in performance compared to pure  $\text{TiO}_2$ , with a slightly higher  $J_{SC}$  value is 0.27 mA/cm<sup>2</sup>. In addition, the  $V_{OC}$  value for this material is higher than pure  $\text{TiO}_2$ , reaching around 0.75 V, before the current starts to decrease significantly. This shows that the addition of a mixture of dye curcuma with  $\text{SiO}_2$  increases the efficiency of charge transfer and stability at a higher voltage [26]. This shows that the dye-curcuma mixture with  $\text{SiO}_2$  significantly increases the efficiency of charge transfer.

For 2L- $\text{SiO}_2$  material, better performance is recorded than all other treatments.  $J_{SC}$  reaches a

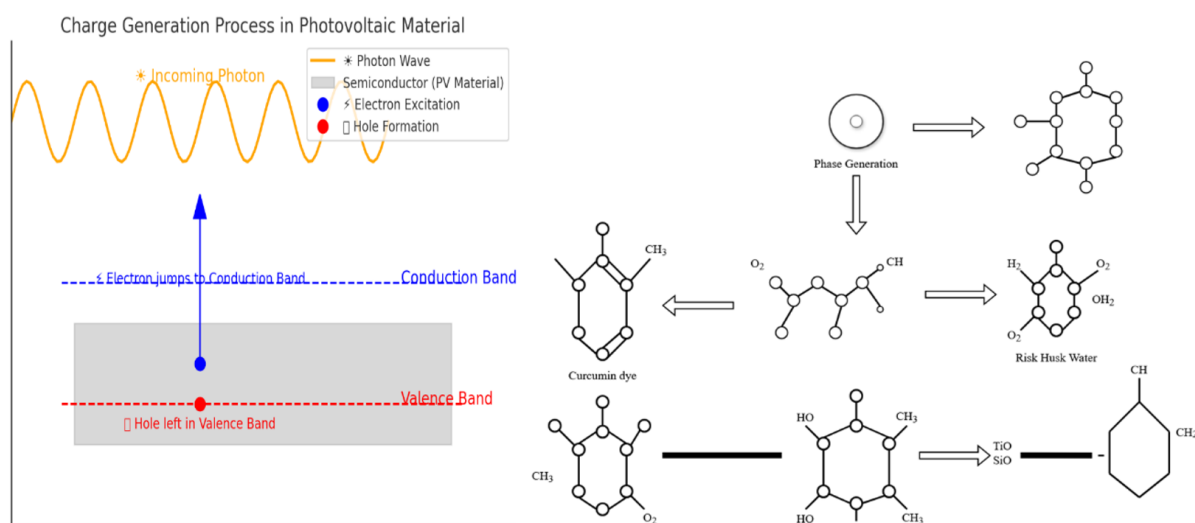
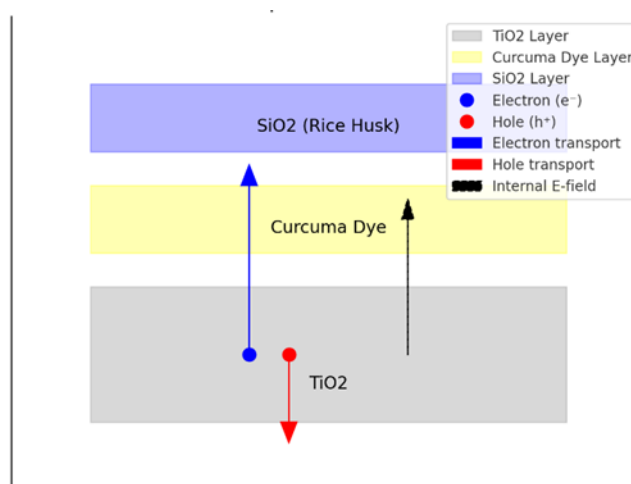


Figure 4. Charge generation in photovoltaic material process.



**Figure 5.** Electron-hole pair formation and transport phenomenon scheme.

maximum value of around  $0.37 \text{ mA/cm}^2$ , which is a significant increase compared to  $\text{TiO}_2$  and 1L- $\text{SiO}_2$ . In addition, this material shows the characteristics of a better  $V_{\text{OC}}$ , with an open circuit voltage that is quite high before a drastic decrease in current. This indicates that the addition of two layers of  $\text{SiO}_2$  produces a more efficient charge transfer and increases carrier charges in the material. However, 1L- $\text{SiO}_2$  material shows less than optimal results compared to 1L- $\text{SiO}_2$ . Although the  $J_{\text{SC}}$  value at low voltage is still quite high ( $0.32 \text{ mA/cm}^2$ ), a decrease in current occurs faster than 1L- $\text{SiO}_2$  when the voltage increases. A sharp decrease in current after  $0.4 \text{ V}$  indicates that excessive layer thickness can inhibit charge transfer, increase recombination of electron holes, and reduce the overall efficiency of the device.

The relationship between the number of layers of mixture of coloring curcuma and  $\text{SiO}_2$  with the efficiency of charge transfer is a crucial aspect in understanding the performance of photovoltaic material. The efficiency of charge transfer is very dependent on the ability of the material to allow electron flow that is not disturbed by high recombination.  $\text{TiO}_2$ , as a basic reference material, shows limitations in maintaining an electric current at high voltage, which reflects the efficiency of low charge transportation. However, there is a significant increase in the efficiency of charge transfer in 1L- $\text{SiO}_2$  material, which is indicated by an increase in the density of  $J_{\text{SC}}$  to  $0.27 \text{ mA/cm}^2$  and a  $V_{\text{OC}}$  of  $0.75 \text{ V}$ . This shows that electrons can move more efficiently before a significant decrease in current.

The best photovoltaic performance is found in 2L- $\text{SiO}_2$  material, with a  $J_{\text{SC}}$  value of  $0.37 \text{ mA/cm}^2$ , which shows the more efficient electron hole transportation pathway and lower resistance in charge transfer. This indicates that the addition of two layers of  $\text{SiO}_2$  made a significant contribution to increasing the efficiency of charge transfer. However, when the number of layers is increased to three (3L- $\text{SiO}_2$ ), there is a negative effect in the form of an increase in charge recombination caused by excessive material thickness. This thickness inhibits the movement of the charge, which causes the current to decrease faster after reaching a voltage of around  $0.4 \text{ V}$ . This finding proves that although the addition of layers can increase charge transfer, there are optimal limits in the number of layers before negative effects, such as higher recombination, begin to reduce the performance of solar cells as a whole. The process of transportation of cargo in photovoltaic material includes four main stages. The first stage is the power generation (Figure 4), where light falls to the surface of the semiconductor such as  $\text{TiO}_2$  lifts electrons from the valence band to the conduction band, forming an electron-hole pair. Only photons who have a minimum energy are equivalent to the gap of the ribbon (band gap) material that can trigger this process.

Furthermore, the electron-hole pair is separated by the internal electric field to prevent the initial recombination (Figure 5). In  $\text{TiO}_2$ -based solar cells modified with dye curcuma and  $\text{SiO}_2$  from rice husk waste,  $\text{TiO}_2$  acts as the main semiconductor, Curcuma increases light absorption, and  $\text{SiO}_2$

stabilizes structure and suppressing the recombination of charge.

The next stage is the charge transportation (Figure 6), where the electron moves to the negative electrode and the hole to the positive electrode through the path with a low resistance. Internal electric fields help separate charges, reduce recombination, and increase the efficiency of charge transfer. However, some charges can experience recombination before reaching the electrode (Figure 7), due to structural defects or atomic irregularities. Material engineering and adding passive layers are needed to suppress this process so that energy conversion remains optimal.

In addition to the charge transfer, the stability of the voltage also plays an important role in determining the performance of photovoltaic material. As the main indicator of voltage stability,  $V_{OC}$  reflects the ability of the material to maintain the voltage before a drastic decrease in current. In  $TiO_2$ , although the  $V_{OC}$  was initially quite good, this material showed a very sharp decrease in current after reaching 0.7 V, which indicated that  $TiO_2$  could not maintain voltage stability at a higher level. Increased voltage stability recorded at 1L- $SiO_2$ , which has a  $V_{OC}$  of 0.75 V, provides better voltage endurance than  $TiO_2$  before the current starts to decrease sharply. 1L- $SiO_2$  shows the best performance in this aspect, with  $V_{OC}$  that remains high before the current starts to decrease, showing the ability of this material to maintain a more stable voltage compared to other materials. However, 1L- $SiO_2$  experienced degradation of voltage stability, because the current began to fall dramatically after reaching 0.4 V, which indicates that the addition of excessive layers increases internal resistance and

accelerates the loss of voltage due to the dominance of recombination of electron holes. This finding confirms that although an increase in layer thickness can increase the efficiency of charge transfer and stability of voltage to a certain point, excessive thickness actually reduces the ability of materials to maintain longer voltage.

Photogeneration of cargo carrier in photovoltaic material is also strongly influenced by the number of  $SiO_2$  layers used, because this layer plays a role in influencing light absorption and its conversion into pairs of holes that can be used in the electricity generation process.  $TiO_2$ , as a reference material, shows the lowest  $J_{SC}$ , which shows that the ability of this material to photogeneration is less optimal. However, with the addition of 1L- $SiO_2$ , photogeneration increases. There was an increase in  $J_{SC}$  from 0.25 to 0.27  $mA/cm^2$ , which means more charge carriers are produced and can contribute to electric current. Peak performance found in 2L- $SiO_2$ , with  $J_{SC}$  reaching 0.37  $mA/cm^2$ , shows that this thickness is an optimal condition to capture light and convert them into holes efficiently. However, when the number of layers increases to 3L- $SiO_2$ , photogeneration is still quite high with  $J_{SC}$  around 0.32  $mA/cm^2$ , but the negative effects begin to appear. Excessive material thickness causes an increase in recombination, reducing the efficiency of cargo carrier transportation, and causing a faster decrease in current compared to 1L- $SiO_2$ . This confirms the balance between material thickness and photogeneration efficiency, where 1L- $SiO_2$  provides the best combination between light absorption, load transportation, and lack of recombination, while excessive thickness, such as in 1L- $SiO_2$ , actually reduces the effectiveness of

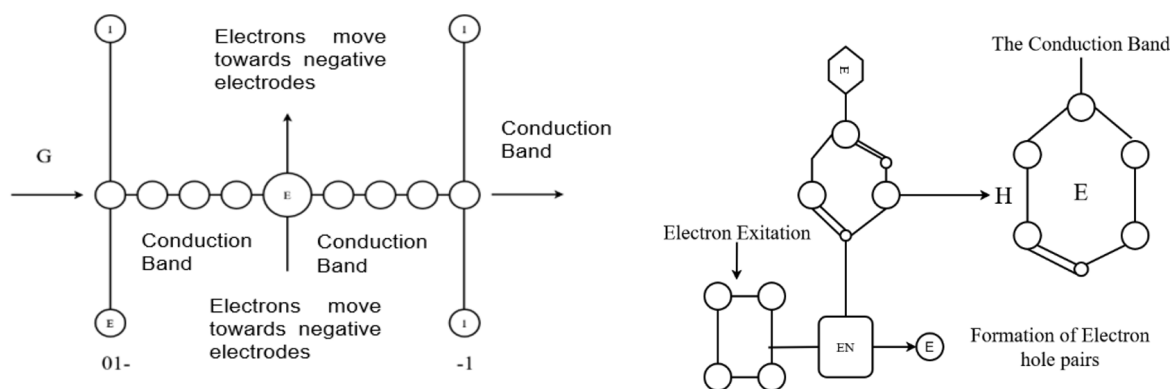


**Figure 6.** Cost transportation process.

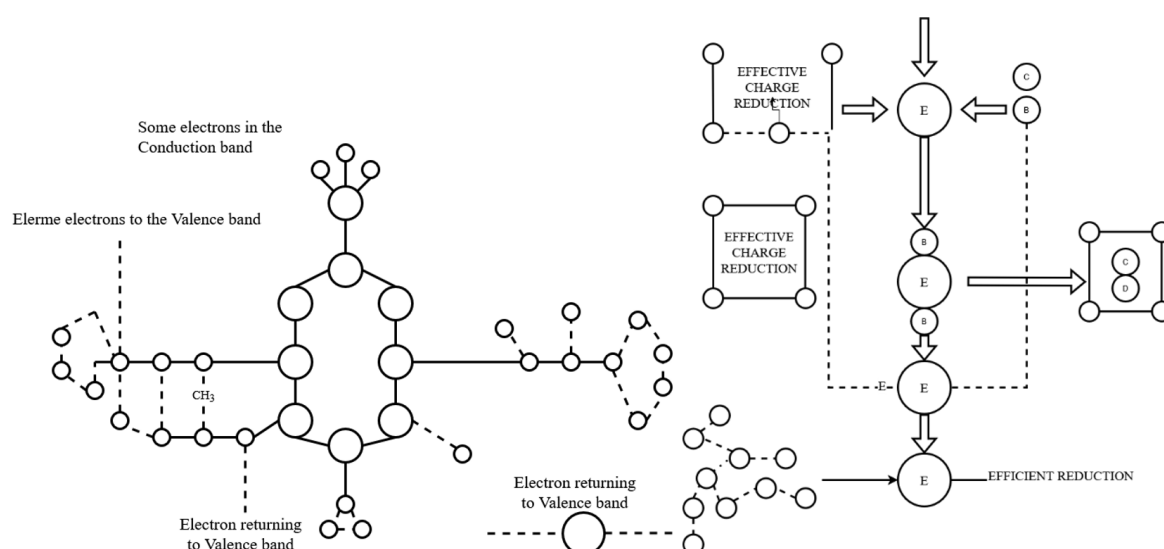


**Figure 7.** Recombination mechanism process.

energy conversion.

### 3.2. SiO<sub>2</sub> Layer Thickness on $P_{MAX}$ , $I_{SC}$ , $V_{OC}$ , $FF$ , and Efficiency Parameters ( $\eta$ ) Solar Cells

Table 1 shows that the 1L-SiO<sub>2</sub> material has a relatively stable performance, with a high maximum power value (0.0347 mW) and an efficiency of 0.0403%. The  $V_{OC}$  recorded is 0.8982 V, which shows the ability of this material in maintaining a good voltage. Filling factor (FF) value of 0.6137 indicates the quality of good filling factors on this device. This characteristic is comparable to TiO<sub>2</sub> material [27].

Conversely, the 2L-SiO<sub>2</sub> material recorded the highest short circuit current ( $I_{SC}$ ) value compared to other compositions, which is 0.0916 mA, which shows a significant increase in short circuit currents. However, the  $V_{OC}$  has decreased to 0.6690 V, which is lower than other compositions. Although the FF remains stable at a value of 0.6156, its efficiency is slightly lower (0.0377%) compared to 1L-SiO<sub>2</sub>. This shows that although the current is higher, other parameter factors are not enough to support to increase the overall efficiency of the device [28]. Although 2L-SiO<sub>2</sub> shows the highest  $J_{SC}$  value (0.037 mA), the efficiency is even lower than 1L-SiO<sub>2</sub> (0.0377% vs. 0.0403%). This is caused by an imbalance of parameters, especially a significant decrease in the  $V_{OC}$  value to 0.6690 V and an increase in the RCT value to 90,388  $\Omega \cdot \text{cm}^2$ . High charge transfer resistance increases the charge recombination, thereby limiting the number of

electrons that succeed in reaching the electrode. Although high  $J_{SC}$  shows effective photogeneration, increased recombination and resistance inhibits the efficiency of overall power conversion. This explanation is now added to strengthen the interpretation of experimental data. Table 1 shows the characteristics of various TiO<sub>2</sub>-based solar material materials.

For 3L-SiO<sub>2</sub> material, although the  $V_{OC}$  value remains equal to 1L-SiO<sub>2</sub> (0.8982 V), the maximum power ( $P_{MAX}$ ) is lower, which is 0.03476 mW. Although the short circuit current ( $I_{SC}$ ) is equal to 1L-SiO<sub>2</sub>, the lower  $V_{MAX}$  value (0.54 V) shows a decrease in performance on the optimal operational voltage side. The efficiency of this material (0.0348%) is also lower than 1L-SiO<sub>2</sub>, indicating that the performance of this material is weaker [28]. Meanwhile, pure TiO<sub>2</sub> material shows similar results with 1L-SiO<sub>2</sub>, which shows that the addition of 1L-SiO<sub>2</sub> does not provide a significant increase to the characteristics of I-V compared to pure TiO<sub>2</sub>.

The highest maximum synchronization  $I_{SC}$  is recorded in 2L-SiO<sub>2</sub> with a value of 0.0916 mA, while the  $I_{SC}$  value at 1L-SiO<sub>2</sub> is relatively lower and parallel to pure TiO<sub>2</sub>. This phenomenon can be explained through optical interactions and electron transportation in material. The SiO<sub>2</sub> layer functions as an anti-reflective layer that reduces the reflection of light from the surface of the solar cells, thereby increasing the amount of light absorbed by the active material (TiO<sub>2</sub>). With a higher photon absorption, more pairs of holes are formed, which



ultimately increase the  $I_{SC}$  value. However, when the thickness of the  $SiO_2$  layer exceeds the optimal limit, this effect begins to reach the point of saturation, and at some point, the layer that is too thick actually functions as a barrier for electron transportation, which causes an increase in recombination of holes. This explains why  $I_{SC}$  reaches its peak at 2L- $SiO_2$ , before finally stagnant or decreases at 3L- $SiO_2$ .

The  $V_{OC}$  is influenced by the quality of the P-N intersection, the level of recombination of holes, as well as the characteristics of the energy barrier formed due to additional layers. The experimental results showed that the highest  $V_{OC}$  was recorded in  $TiO_2$  and 1L- $SiO_2$  with a value of 0.8982 V, whereas in 2L- $SiO_2$ , the  $V_{OC}$  dropped significantly to 0.6690 V. The decrease in the  $V_{OC}$  was most likely due to an increase in carrier recombination due to excessive layer thickness. At 1L- $SiO_2$ , the  $SiO_2$  layer is still thin enough so that it does not inhibit electron transportation significantly and can even increase energy resistance, which reduces recombination. However, at 1L- $SiO_2$ , a greater layer thickness increases the likelihood of carrier recombination before reaching the electrode, which causes a decrease in the  $V_{OC}$ . When the thickness of the layer reaches 3L- $SiO_2$ , the  $V_{OC}$  returns to 0.8982 V, shows that electron transportation in the layer may have reached the balance point, although the negative impact on maximum power ( $P_{MAX}$ ) still exists.

The highest  $P_{MAX}$  value occurs at  $TiO_2$  with a value of 0.04033 mW, while at 2L- $SiO_2$ ,  $P_{MAX}$  decreases slightly to 0.0377 mW, and at 1L- $SiO_2$ ,  $P_{MAX}$  dropped further to 0.03476 mW. This decrease in  $P_{MAX}$  is caused by the effect of the thickness of the  $SiO_2$  layer on other parameters, especially  $V_{OC}$  and the efficiency of cargo transportation. Although the  $I_{SC}$  at 1L- $SiO_2$  increases, a significant decrease in the  $V_{OC}$  causes the maximum power not to increase proportionally. In 1L- $SiO_2$ , although the  $V_{OC}$  is again increasing, the effect of increasing internal resistance and the possibility of the effect of capacitance due to greater layer thickness resulting in a decrease in  $P_{MAX}$ . This shows that there is an optimal limit in the thickness of the  $SiO_2$  layer, where a layer that is too thin does not provide sufficient optical benefits, while the layer that is too thick actually reduces the

**Table 1.** Characteristics of I-V various compositions of  $TiO_2$  material.

Sample	Characteristics I-V						
	Pmax (mW)	Isc (mA)	Voc (V)	FF	Imax (mA)	Vmax (V)	h (%)
TiO	0.040334059	0.07317087	0.898216392	0.613695208	0.05307113	0.76	0.000403341
1L-SiO <sub>2</sub>	0.034763029	0.07317087	0.898216392	0.613695208	0.05307113	0.76	0.000403341
2L-SiO <sub>2</sub>	0.037722423	0.09159547	0.669021152	0.615581754	0.08573278	0.44	0.000377224
3L-SiO <sub>2</sub>	0.034763062	0.07317087	0.898216392	0.613695208	0.06437604	0.54	0.000347631

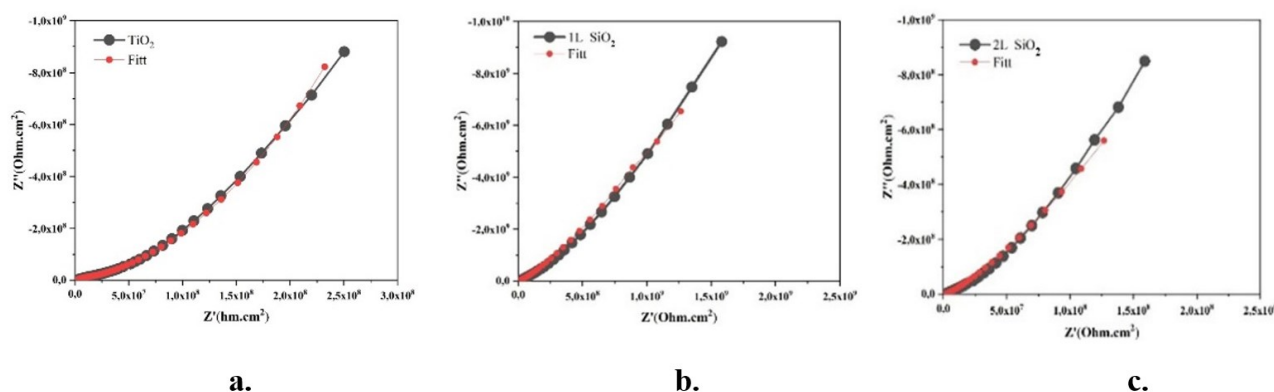


**Figure 8.** Material complex impedance curve of (a)  $\text{TiO}_2$ , (b) 1L-  $\text{SiO}_2$ , and (c) 2L-  $\text{SiO}_2$ .

efficiency of cargo transportation in the material.

The FF value is relatively stable throughout the composition, ranging from 0.6137 to 0.6156. This stability indicates that the characteristics of the intersection diode in solar cells are not significantly affected by the thickness of the  $\text{SiO}_2$  layer. The stable FF value indicates that the series resistance and shunt resistance in the system remain constant even though there are variations in the thickness of the  $\text{SiO}_2$  layer. Low series resistance allows efficient charge transfer, while low shunt resistance prevents unwanted current leakage. Therefore, although other parameters such as  $V_{OC}$  and  $I_{SC}$  experience significant changes with an increase in the thickness of the  $\text{SiO}_2$  layer, the FF value remains stable because the internal resistance of the device does not experience significant changes.

The highest efficiency was recorded at 1L- $\text{SiO}_2$  with a value of 0.0403%, while the efficiency at 2L- $\text{SiO}_2$  dropped to 0.0377%, and lower at 3L- $\text{SiO}_2$ , which was 0.0348%. Although 1L- $\text{SiO}_2$  shows a high  $I_{SC}$ , a significant decrease in the  $V_{OC}$  causes overall efficiency to decrease. In 1L- $\text{SiO}_2$ , although the  $V_{OC}$  increases again, the  $P_{MAX}$  remains low, which indicates that its efficiency is still lower. This phenomenon indicates that optimal efficiency occurs in layers thickness that is not too thin or too thick. A layer that is too thin cannot provide sufficient optical effects to increase light absorption, while a layer that is too thick increases resistance and recombination of carriers, thereby reducing the number of electrons that contribute to electric current. Therefore, the selection of additional layers thickness such as  $\text{SiO}_2$  is very crucial in increasing the efficiency of  $\text{TiO}_2$ -based solar cells. The efficiency of solar cells in this study

is indeed lower than DSSC -based synthetic dyes such as N719 (~ 7%). However, this value is still in the range of previous reports for natural dyes (0.1% –0.7%) [29]. It is necessary to optimize further on the structure of the electrode and the dyeing condition

### 3.3 $\text{SiO}_2$ Layer Variation on Resistance and Capacitance of Solar Cells

Figure 5 shows the complex impedance curve for  $\text{TiO}_2$ , 1L- $\text{SiO}_2$ , and 2L- $\text{SiO}_2$  material variations. This curve analysis allows the evaluation of the effects of variations in a mixture of dyes with  $\text{SiO}_2$  on resistance and capacitance in solar cells.

Figure 8 shows that the variation of the  $\text{TiO}_2$  material produces a larger impedance arches, which indicates a high charge transfer resistance (RCT) of  $12,486 \Omega \cdot \text{cm}^2$ , which has an impact on the efficiency of the load transfer that is less than optimal [29]. The first capacitance (C1) of 5.86 F shows a good charge storage capacity, although it can still be optimized, while the series resistance (RS) recorded at  $25.10 \Omega \cdot \text{cm}^2$  is still within an acceptable limit for the photovoltaic application, although not ideal. Overall, although  $\text{TiO}_2$  is able to maintain a good voltage, the high charge resistance of charge inhibits the efficiency of the electron hole transfer, which ultimately has a negative impact on the overall performance of solar cells.

Conversely, the 1L- $\text{SiO}_2$  material shows a smaller impedance curve compared to  $\text{TiO}_2$ , which indicates a decrease in charge transfer resistance with a lower RCT value, which However, the first capacitance is reduced to 1.07 F, indicating a lower charge storage capacity compared to  $\text{TiO}_2$ , which has the potential to affect the stability of

performance in the long run. A significant increase in the series resistance to  $96.91 \Omega \cdot \text{cm}^2$  can inhibit the flow of charge and reduce the efficiency of output power. Therefore, although the efficiency of charge transfer increases with a decrease in RCT, increased series resistance is the main obstacle in improving the overall performance of solar cells [30].

The 1L-SiO<sub>2</sub> material shows a different pattern, where the impedance arches are smaller at first, but increase sharply in high resistance. The RCT value increases dramatically to  $90,388 \Omega \cdot \text{cm}^2$ , much higher than TiO<sub>2</sub> and 1L-SiO<sub>2</sub>, which shows an increase in charge transfer resistance that can increase the level of charge recombination. However, capacitance increased to 3.68 F, which allows this material to store more charges than 1L-SiO<sub>2</sub>, although it is still lower than TiO<sub>2</sub>. The advantage of 1L-SiO<sub>2</sub> lies in a significant decrease in the series resistance recorded at  $16.78 \Omega \cdot \text{cm}^2$ , much lower than TiO<sub>2</sub> and 1L-SiO<sub>2</sub>, which shows that the charge transfer in electric paths is more efficient. However, the high RCT value results in the transfer of electron holes that are less efficient and increase the possibility of charge recombination, which can inhibit the efficiency of solar cells. Thus, although 1L-SiO<sub>2</sub> shows the advantage in terms of lower series resistance, a significant increase in charge transfer resistance can inhibit the efficiency of charge transfer and reduce the overall performance of the device.

In the TiO<sub>2</sub> material, the curvature of the large impedance in the nyquist curve shows a high RCT, with a value of  $12,486 \Omega \cdot \text{cm}^2$ . This resistance is a major factor in inhibition of charge movements, which leads to low charge transfer efficiency, so that it has a negative impact on the overall performance of the photovoltaic device. Although this material can maintain the voltage properly, limitations in the transfer of charge reduce their efficiency, especially for applications that require high speed in electron transfer. In terms of capacitance, the C1 value of 5.86 F shows a fairly good charge storage capacity, which contributes to the stability of the system, although there is still potential for further optimization. On the other hand, series resistance (RS) of  $25.10 \Omega \cdot \text{cm}^2$  is within reasonable limits, but this value is not low enough to support maximum charge transfer

efficiency.

When one layer of SiO<sub>2</sub> (1L-SiO<sub>2</sub>) is added, the RCT value decreases to  $10.501 \Omega \cdot \text{cm}^2$ , which shows an increase in the efficiency of charge transfer, because electrons can move more easily compared to pure TiO<sub>2</sub>. However, the decrease in RCT is accompanied by a decrease in the first capacitance (C1), which decreased to 1.07 F. This shows that although the efficiency of the charge transfer increases, the ability of the material in storing charges decreases. As a result, although the load transfer becomes more efficient, the capacity of charge storage can be a long-term challenge. In addition, series resistance increases significantly to  $96.91 \Omega \cdot \text{cm}^2$ , which can limit the flow of charge and reduce the efficiency of the device output power. Therefore, despite the decline in RCT in 1L-SiO<sub>2</sub> increases the efficiency of charge transfer, increased series resistance and decreased capacitance must be taken into account to ensure optimal performance [31].

When the material is further modified with the addition of two layers of SiO<sub>2</sub> (2L-SiO<sub>2</sub>), the impedance pattern becomes more complex, with a nyquist curve that was initially smaller but showed a sharp increase in higher resistance values. The most significant increase is in RCT which reaches  $90,388 \Omega \cdot \text{cm}^2$ , which shows that the charge resistance is greater. This increases the likelihood of recombination of charges, which can reduce the efficiency of overall energy conversion. However, in contrast to 1L-SiO<sub>2</sub>, capacitance at 1L-SiO<sub>2</sub> increased to 3.68 F, which shows that the charge capacity is better than 1L-SiO<sub>2</sub>, although it is still lower than pure TiO<sub>2</sub>. The main advantage of the 2L-SiO<sub>2</sub> lies in a significant decrease in the series resistance which now reaches  $16.78 \Omega \cdot \text{cm}^2$ , which shows a more efficient charge transfer pathway, so as to increase the output power of the device [32]. Although the series resistance decreases and capacitance increases, the high RCT value remains the main resistance because it can increase the recombination.

#### 4. CONCLUSIONS

The thickness of the SiO<sub>2</sub> layer has a significant effect on the performance of TiO<sub>2</sub>-based solar cells. The addition of one layer of SiO<sub>2</sub> (1L-SiO<sub>2</sub>) has

succeeded in increasing the  $J_{SC}$  and  $V_{OC}$  compared to pure  $TiO_2$ , which shows an increase in the efficiency of charge transfer. Meanwhile, the addition of two layers of  $SiO_2$  (2L- $SiO_2$ ) gave the best performance, reflected in the highest  $J_{SC}$  value of 0.37 MA/cm<sup>2</sup> and optimal charge transfer efficiency. However, the addition of three layers of  $SiO_2$  (3L- $SiO_2$ ) actually resulted in a decrease in overall performance, caused by an increase in charge transfer resistance and recombination of electron holes, which reduces the efficiency of the device. Based on parameter I-V analysis, layer 1L- $SiO_2$  shows the highest efficiency of 0.0403% and the best maximum power. The addition of two layers of  $SiO_2$  (2L- $SiO_2$ ) produces a higher  $J_{SC}$  value than 1L- $SiO_2$ , but the decline in the  $V_{OC}$  value causes the overall efficiency to be lower. In layer three (3L- $SiO_2$ ), although the  $V_{OC}$  increases again, efficiency remains decreased due to an increase in internal resistance. The FF shows stability throughout the composition of the  $SiO_2$  layer, which indicates that internal resistance is not significantly affected by the variation of the thickness of the  $SiO_2$  layer. The results of complex impedance analysis indicate that pure  $TiO_2$  has the highest RCT of 12,486  $\Omega \cdot cm^2$ , which inhibits the efficiency of cargo transportation in material. The addition of 1L- $SiO_2$  reduces the RCT value to 10.501  $\Omega \cdot cm^2$ , which increases the efficiency of charge transfer, although the series resistance (RS) increases. At 1L- $SiO_2$ , although the hospital value decreased to 16.78  $\Omega \cdot cm^2$ , the RCT value increased dramatically to 90.388  $\Omega \cdot cm^2$ , which contributed to an increase in the recombination of electron holes and reduced the efficiency of energy conversion. The addition of  $SiO_2$  layers increases the efficiency of charge transfer to reach the optimal point at 1L- $SiO_2$ , but excessive layer thickness can reduce efficiency due to increased internal resistance and greater charge recombination.

## AUTHOR INFORMATION

### Corresponding Author

**Tulus Subagyo** — Department of Mechanical Engineering, Yudharta University, Pasuruan-67162 (Indonesia); Department of Mechanical Engineering, Brawijaya University, Malang-65145 (Indonesia);

 [orcid.org/0009-0002-8511-6549](https://orcid.org/0009-0002-8511-6549)

Email: [tulus@yudharta.ac.id](mailto:tulus@yudharta.ac.id)

## Authors

**Denny Widhiyanuriyawan** — Department of Mechanical Engineering, Brawijaya University, Malang-65145 (Indonesia);

 [orcid.org/0000-0001-5729-4212](https://orcid.org/0000-0001-5729-4212)

**Agung Sugeng Widodo** — Department of Mechanical Engineering, Brawijaya University, Malang-65145 (Indonesia);

 [orcid.org/0000-0002-5331-9950](https://orcid.org/0000-0002-5331-9950)

**I Nyoman Gede Wardana** — Department of Mechanical Engineering, Brawijaya University, Malang-65145 (Indonesia);

 [orcid.org/0000-0003-3146-9517](https://orcid.org/0000-0003-3146-9517)

## Author Contributions

Conceptualization, Writing – Original Draft Preparation, Writing – Review & Editing, T. S. and I N. G. Wardana; Methodology, Validation, Formal Analysis, Investigation, Resources, Data Curation, Visualization, Project Administration, and Funding Acquisition, T. S.; Software, T. S. and D. W.; Supervision, D. W., A. S. W., and I. N. G. W.

## Conflicts of Interest

The authors declare that they have no conflict of interest in relation to this research, whether financial, personal, authorship or otherwise, that could affect the research and its results presented in this paper.

## ACKNOWLEDGEMENT

We would like to express our gratitude to Central Laboratory, State University of Malang and Lab Riset Terpadu (LRT) Brawijaya University.

## REFERENCES

- [1] M. E. Wilson, M. G. Rukh, and M. A. Ashraf. (2021). "The role of nanotechnology, based on carbon nanotubes in water and wastewater treatment". *Desalination and Water Treatment*. **242** : 12-21. [10.5004/dwt.2021.27568](https://doi.org/10.5004/dwt.2021.27568).
- [2] G. Yashni, A. A. Al-Gheethi, R. M. S. R. Mohamed, S. N. H. Arifin, and N. H.

- Hashim. (2019). "Synthesis of nanoparticles using biological entities: an approach toward biological routes". *Desalination and Water Treatment*. **169** : 152-165. [10.5004/dwt.2019.24666](https://doi.org/10.5004/dwt.2019.24666).
- [3] Widjanarko, N. Alia, P. Fengky Adie, U. Pondi, and E. Puspitasari. (2024). "Sustainable Power Generation through Dual -Axis Solar Tracking for Off Grid 100Wp Photovoltaic Systems". *Evrinata: Journal of Mechanical Engineering*. 118-124. [10.70822/evrimata.v1i04.63](https://doi.org/10.70822/evrimata.v1i04.63).
- [4] B. Sun, F. Zhao, Y. Cheng, C. Shao, M. Sun, M. Yi, Y. Wang, X. Wang, S. Zhu, and X. Cai. (2023). "Synthesis and characterization of polymetallic Fe-Co-Ni-S nanocomposite displaying high adsorption capacity for Rhodamine B dye". *Desalination and Water Treatment*. **303** : 200-211. [10.5004/dwt.2023.29758](https://doi.org/10.5004/dwt.2023.29758).
- [5] N. Farooq, P. Kallem, Z. ur Rehman, M. Imran Khan, R. Kumar Gupta, T. Tahseen, Z. Mushtaq, N. Ejaz, and A. Shanableh. (2024). "Recent trends of titania (TiO<sub>2</sub>) based materials: A review on synthetic approaches and potential applications". *Journal of King Saud University - Science*. **36** (6). [10.1016/j.jksus.2024.103210](https://doi.org/10.1016/j.jksus.2024.103210).
- [6] V. Seiththanabutar, N. Chumwangwapee, A. Saksri, and T. Wongwuttanasatian. (2023). "Potential investigation of combined natural dye pigments extracted from ivy gourd leaves, black glutinous rice and turmeric for dye-sensitized solar cell". *Heliyon*. **9** (11): e21533. [10.1016/j.heliyon.2023.e21533](https://doi.org/10.1016/j.heliyon.2023.e21533).
- [7] M. K. Hossain, M. F. Pervez, M. N. H. Mia, A. A. Mortuza, M. S. Rahaman, M. R. Karim, J. M. M. Islam, F. Ahmed, and M. A. Khan. (2017). "Effect of dye extracting solvents and sensitization time on photovoltaic performance of natural dye sensitized solar cells". *Results in Physics*. **7** : 1516-1523. [10.1016/j.rinp.2017.04.011](https://doi.org/10.1016/j.rinp.2017.04.011).
- [8] N. Khansili and P. M. Krishna. (2022). "Curcumin functionalized TiO<sub>2</sub> modified bentonite clay nanostructure for colorimetric Aflatoxin B1 detection in peanut and corn". *Sensing and Bio-Sensing Research*. **35**. [10.1016/j.sbsr.2022.100480](https://doi.org/10.1016/j.sbsr.2022.100480).
- [9] A. Fall, N. L. Botha, H. E. Ahmed Mohamed, K. J. Cloete, J. Sackey, B. D. Ngom, and M. Maaza. (2023). "Photocatalytic response of bio-engineered nano-TiO<sub>2</sub> via *Adansonia digitata* leaves' natural extract". *Materials Today: Proceedings*. [10.1016/j.matpr.2023.09.127](https://doi.org/10.1016/j.matpr.2023.09.127).
- [10] S. C. Ezike, C. N. Hyelnasinyi, M. A. Salawu, J. F. Wansah, A. N. Ossai, and N. N. Agu. (2021). "Synergistic effect of chlorophyll and anthocyanin Co-sensitizers in TiO<sub>2</sub>-based dye-sensitized solar cells". *Surfaces and Interfaces*. **22**. [10.1016/j.surfin.2020.100882](https://doi.org/10.1016/j.surfin.2020.100882).
- [11] M. Yavarzadeh, F. Nasirpour, L. J. Foruzin, and A. Pourandarjani. (2024). "Photocurrent response loss of dye sensitized solar cells owing to top surface nanogras growth and bundling of anodic TiO(2) nanotubes". *Heliyon*. **10** (2): e24247. [10.1016/j.heliyon.2024.e24247](https://doi.org/10.1016/j.heliyon.2024.e24247).
- [12] A. Błaszczuk, K. Joachimiak-Lechman, S. Sady, T. Tański, M. Szindler, and A. Drygała. (2021). "Environmental performance of dye-sensitized solar cells based on natural dyes". *Solar Energy*. **215** : 346-355. [10.1016/j.solener.2020.12.040](https://doi.org/10.1016/j.solener.2020.12.040).
- [13] M. Kozin, M. S. Mustapa, Y. A. Winoko, and E. Faizal. (2023). "Solar Charger Controller Efficiency Analysis of Type Pulse Width Modulation (PWM) and Maximum Power Point Tracking (MPPT)". *Asian Journal Science and Engineering*. **1** (2). [10.51278/ajse.v1i2.546](https://doi.org/10.51278/ajse.v1i2.546).
- [14] V. Jagadeeswara Reddy, M. Fairusham Ghazali, and S. Kumarasamy. (2024). "Innovations in phase change materials for diverse industrial applications: A comprehensive review". *Results in Chemistry*. **8**. [10.1016/j.rechem.2024.101552](https://doi.org/10.1016/j.rechem.2024.101552).
- [15] S. Kumar, S. J, S. S. Sharma, H. Paliwal, G. Manikanta, J. Giri, S. M. M. Hasnain, and R. Zairov. (2024). "Developments, challenges, and projections in solar battery charging in India". *Results in Engineering*. **24**. [10.1016/j.rineng.2024.103248](https://doi.org/10.1016/j.rineng.2024.103248).
- [16] Reynaldo and Y. A. Winoko. (2024). "ESP 8266-Based Car Battery Current And Voltage Monitoring Design". *Evrinata: Journal of*



- Mechanical Engineering*. 51-56. [10.70822/evrmata.vi.43](https://doi.org/10.70822/evrmata.vi.43).
- [17] J. A. Abdalla, R. A. Hawileh, A. Bahurudeen, Jittin, K. I. Syed Ahmed Kabeer, and B. S. Thomas. (2023). "Influence of synthesized nanomaterials in the strength and durability of cementitious composites". *Case Studies in Construction Materials*. **18**. [10.1016/j.cscm.2023.e02197](https://doi.org/10.1016/j.cscm.2023.e02197).
- [18] B. Irawan, S. Hadi, S. Hadi, and K. Witono. (2023). "Analysis of The Cooling Spray System for Hot Pool Water With An Electricity Source from Solar Cells". *Journal of Evrimata: Engineering and Physics*. 31-37. [10.70822/journalofevrmata.vi.10](https://doi.org/10.70822/journalofevrmata.vi.10).
- [19] P. Suresh, J. J. Vijaya, T. Balasubramaniam, and L. John Kennedy. (2016). "Synergy effect in the photocatalytic degradation of textile dyeing waste water by using microwave combustion synthesized nickel oxide supported activated carbon". *Desalination and Water Treatment*. **57** (8): 3766-3781. [10.1080/19443994.2014.989276](https://doi.org/10.1080/19443994.2014.989276).
- [20] R. Mahadevan, S. Palanisamy, and P. Sakthivel. (2023). "Role of nanoparticles as oxidation catalyst in the treatment of textile wastewater: Fundamentals and recent advances". *Sustainable Chemistry for the Environment*. **4**. [10.1016/j.scenv.2023.100044](https://doi.org/10.1016/j.scenv.2023.100044).
- [21] W. Xie, T. Cheng, C. Chen, C. Sun, L. Qi, and Z. Zhang. (2020). "Optimizing and modeling Cu(II) removal from simulated wastewater using attapulgite modified with Keggin ions with the aid of RSM, BP-ANN, and GA-BP". *Desalination and Water Treatment*. **207** : 270-286. [10.5004/dwt.2020.26429](https://doi.org/10.5004/dwt.2020.26429).
- [22] A. Asrori, M. F. S. Alfarisyi, A. M. Zainuri, and E. Naryono. (2024). "Characterization of the Bioenergy Potential of Corncob and Rice Husk mixtures in Biochar Briquettes". *Evrímata: Journal of Mechanical Engineering*. 14-20. [10.70822/evrmata.vi.22](https://doi.org/10.70822/evrmata.vi.22).
- [23] M. Ali and M. A. Tindyala. (2018). "Thermoanalytical studies on acid-treated rice husk and production of some silicon based ceramics from carbonised rice husk". *Journal of Asian Ceramic Societies*. **3** (3): 311-316. [10.1016/j.jascer.2015.06.003](https://doi.org/10.1016/j.jascer.2015.06.003).
- [24] N. N. Nguyen, A. V. Nguyen, and M. Konarova. (2025). "Converting rice husk biomass into value-added materials for low-carbon economies: Current progress and prospect toward more sustainable practices". *Journal of Environmental Chemical Engineering*. **13** (2). [10.1016/j.jece.2025.115499](https://doi.org/10.1016/j.jece.2025.115499).
- [25] E. Puspitasari, Y. Eko, A. Lisa, and A. Nila. (2024). "Small PLTS Off Grid 240 WP On Residential House Rooftop". *Evrímata: Journal of Mechanical Engineering*. 81-87. [10.70822/evrmata.v1i03.56](https://doi.org/10.70822/evrmata.v1i03.56).
- [26] R. M. Mohamed, I. A. Mkhaliid, M. Abdel Salam, and M. A. Barakat. (2013). "Zeolite Y from rice husk ash encapsulated with Ag-TiO<sub>2</sub>: characterization and applications for photocatalytic degradation catalysts". *Desalination and Water Treatment*. **51** (40-42): 7562-7569. [10.1080/19443994.2013.775671](https://doi.org/10.1080/19443994.2013.775671).
- [27] J. Hayfron, S. Jaaskelainen, and S. Tetteh. (2025). "Synthesis of zeolite from rice husk ash and kaolinite clay for the removal of methylene blue from aqueous solution". *Heliyon*. **11** (1): e41325. [10.1016/j.heliyon.2024.e41325](https://doi.org/10.1016/j.heliyon.2024.e41325).
- [28] Y. Kusumawati, A. S. Hutama, D. V. Wellia, and R. Subagyo. (2021). "Natural resources for dye-sensitized solar cells". *Heliyon*. **7** (12): e08436. [10.1016/j.heliyon.2021.e08436](https://doi.org/10.1016/j.heliyon.2021.e08436).
- [29] I. Saukani, E. Nuraini, A. Sukoco Heru Sumarno, R. Tri Turani Saptawati, I. Islahunufus, and F. I. Sifaunnufus Ms. (2024). "Buck-boost converter in photovoltaics for battery chargers". *Journal of Evrimata: Engineering and Physics*. 85-89. [10.70822/journalofevrmata.vi.26](https://doi.org/10.70822/journalofevrmata.vi.26).
- [30] R. A. Bakar, R. Yahya, and S. N. Gan. (2016). "Production of High Purity Amorphous Silica from Rice Husk". *Procedia Chemistry*. **19** : 189-195. [10.1016/j.proche.2016.03.092](https://doi.org/10.1016/j.proche.2016.03.092).
- [31] S. Chavan, D. Mitra, and A. Ray. (2024). "Harnessing rice husks: Bioethanol production for sustainable future". *Current*

- Research in Microbial Sciences*. **7** : 100298. [10.1016/j.crmicr.2024.100298](https://doi.org/10.1016/j.crmicr.2024.100298).
- [32] I. G. Bawa Susana, I. B. Alit, and I. D. K. Okariawan. (2023). "Rice husk energy rotary dryer experiment for improved solar drying thermal performance on cherry coffee". *Case Studies in Thermal Engineering*. **41**. [10.1016/j.csite.2022.102616](https://doi.org/10.1016/j.csite.2022.102616).